Climate Services 30 (2023) 100372

Contents lists available at ScienceDirect

Climate Services

journal homepage: www.elsevier.com/locate/cliser

Climate change scenarios in use: Heat stress in Switzerland

A. Casanueva [a,b,c,*], S. Kotlarski [a], M.A. Liniger [a], C. Schwierz [a], A.M. Fischer [a]

[a] Federal Office of Meteorology and Climatology MeteoSwiss, Zurich-Airport, Switzerland
[b] Dept. Matemática Aplicada y Ciencias de la Computación (MACC), Universidad de Cantabria, Santander, Spain
[c] Grupo de Meteorología y Computación (Unidad Asociada al CSIC por el IFCA), Santander, Spain

HIGHLIGHTS

- Accentuated increase of heat stress in Switzerland under the moderate and strong emission scenarios towards the end of the century.
- High heat stress 3–5 times more frequent for the strong emission scenario compared to the mitigation scenario.
- Climate analogs based on heat stress spells largely depend on the emission scenario.
- The inclusion of humidity narrows down the localization of good climate analogs.

GRAPHICAL ABSTRACT

Framework of the present study, which builds upon the CH2018 scenarios (scribbles for the products were designed by zeichenfabrik.ch) and extends to climate analogs for heat stress. (Other illustrations and photos are licensed under Creative Commons Zero, Public Domain Dedication).

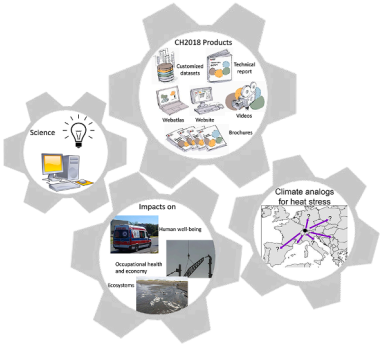

ARTICLE INFO

Keywords:
Heat stress
Climate change
Climate services
Climate analogs
Switzerland
Climate scenarios

ABSTRACT

Under hot conditions the human body is able to regulate its core temperature via sweat evaporation, but this ability is reduced when air humidity is high. These conditions of high temperature and high humidity invoke heat stress which is a major problem for humans, in particular for vulnerable groups of the population and people under physical stress (e.g. heavy duty work without appropriate cooling systems). It is generally expected that the frequency, duration and magnitude of such unfavorable conditions will increase with further climate warming. In this respect, climate services play a crucial role by putting together climatological information and adaptation solutions to reduce future heat stress. We here assess the recently developed CH2018 scenarios for Switzerland (https://www.climate-scenarios.ch) in terms of heat stress conditions including their future projections. For this purpose, we characterize future extreme heat conditions with the use of climate analogs. By doing so, we attempt to produce more accessible climate information which might foster the use and understanding of regional-scale climate scenarios.

Here heat stress is expressed through the Wet Bulb Temperature (TW), which is a relatively simple proxy for heat stress on the human body and which depends non-linearly on temperature and humidity. It is assessed in terms of single-day events and heat stress spells. Projections based on the CH2018 scenarios indicate increasing heat stress over Switzerland, which is accentuated towards the end of the century. High heat stress conditions

* Corresponding author.
E-mail address: ana.casanueva@unican.es (A. Casanueva).

https://doi.org/10.1016/j.cliser.2023.100372
Received 10 June 2022; Received in revised form 18 January 2023; Accepted 11 April 2023
Available online 25 April 2023

might be about 3–5 times more frequent for an emission scenario without mitigation (RCP 8.5) than for the mitigation scenario (RCP 2.6) by the end of the 21st century. The projected increase of heat stress results in more and longer heat stress spells, thus highlighting the importance of timely and precise prevention strategies in the context of heat-health action plans. Spatial climate analogs based on heat stress spells in Switzerland greatly vary depending on the emission scenario and are found in Central Europe under a mitigation scenario and in southern Europe under unmitigated warming.

Practical implications

Climate service providers around the world are making large efforts to produce national and regional climate change scenarios. The vast amount of information produced is, however, very often underexploited. This is, on the one hand, due to too complex formats and technical requirements, on the other hand, it is due to the diverse spectrum of stakeholder needs and challenging communication. The projected numbers frequently provide too little information for the general population and stakeholders and some strategies are required to communicate climate scenarios in a user-friendly manner. For this reason, the quality of climate services relies both on a proper incorporation of a rigorous and robust scientific assessment and a proper incorporation of user-needs in an inter- and trans-disciplinary setting.

In the framework of the Swiss climate change scenarios CH2018 (CH2018, 2018, Fischer et al. 2022), a big step was made to improve upon previous scenarios in terms of user-oriented climate information, both qualitatively and quantitatively (see e.g. CH2018 products in Fig. 1). Heat is considered as a primary climate hazard in Switzerland. Accordingly, CH2018 made available a new dataset which, among others, includes metrics relevant for heat-stress (INDEX-LOCAL product in CH2018, 2018, Fischer et al. 2022), to give support to decision-makers regarding heat-related impacts, such as human well-being, occupational health, labour productivity and heat-related effects on ecosystems. In this work we add to the existing CH2018 products and further exploit the INDEX-LOCAL dataset. More precisely, we examine heat stress spells and propose climate analogs as a tool to identify places with recently experienced heat stress conditions similar to the future projections of the place of interest (Fig. 1). This way, climate projections connect with personal experience and historical climate situations, which is essential for the engagement of the users and for establishing a bidirectional exchange between products and impacted sectors.

Data availability

Data will be made available on request.

Introduction

Very high temperatures during the night and day greatly affect human health and well-being. Heat exposure can raise the core body temperature and thus cause heat-related illnesses (Petitti et al. 2016, Mora et al. 2017) and impact labour productivity (Kjellstrom et al. 2009, 2018) and, consequently, the economic output (García-León et al. 2021). The effect of temperature on the human body is enhanced by other meteorological conditions, such as high relative humidity, exposure to radiation or lack of wind. When the external temperature is high, the only way for the body to stay at a healthy core temperature is through the loss of heat via sweat evaporation. However, high external air humidity and certain clothing (e.g., protective clothing worn in particular jobs) limit sweat evaporation, forcing core body temperature to rise (UNDP, 2016). Under such circumstances, the combination of external heat exposure and internal heat production generated from metabolic processes can provoke heat stress (Xiang et al., 2014). High heat stress during single days is relevant for vulnerable groups of the population, especially if people are not acclimatized (e.g., in late spring or beginning of summer). However, the negative impacts of heat stress become worse under prolonged periods of high heat exposure (Ciuha et al., 2019). It has a cumulative effect since, for instance, people in cities might not recover from the daytime heat at night due to the urban heat island and might subsequently not be able to handle extreme heat the following day (Perkins, 2015). Analyzing the evolution of such conditions becomes crucial to protect population health and prevent other heat-related impacts at different time-scales. In this work, we additionally show how learning from meteorological heat warnings might foster the use of climate change scenarios.

In a climate change context, heat stress is projected to continuously increase towards the end of the century (Willett and Sherwood 2010, Zhao et al. 2015, Knutson and Ploshay 2016, Coffel et al. 2018, Li et al. 2018, Matthews 2018), mainly as a direct consequence of the increase in mean temperatures (Fischer and Schär, 2010). Heat stress constitutes an important threat in densely populated areas, for instance, India, Southeast Asia, the Arabian Gulf and the Sahel (Zhao et al. 2015, Pal and Eltahir 2016, Rohini et al. 2016, Mora et al. 2017, Moda et al. 2019, Suarez-Gutierrez et al. 2020). Also in Europe, temperature extremes and heat stress are projected to increase towards the end of the 21st century, as well as the duration and frequency of heat waves and warm spells (Jacob et al. 2014, Horton et al. 2016, King and Karoly 2017, Seneviratne et al. 2021). The number of days with high heat stress risk might become more frequent in large areas of the continent, including Central and northern Europe, especially for people active in the sun (Casanueva et al., 2020). Economic losses due to reduced labour productivity are especially important in southern Europe (>50% of working hours lost in some locations in Spain, Italy, Greece and Cyprus) and might range between 5 and 20% in Lugano (Switzerland) under the strong emission scenario by the end of the century (Casanueva et al., 2020).

The obvious importance of elevated heat stress as a main climate hazard highlights the need for coordinated plans to develop mitigation and adaptation actions based on scientifically sound science and the interaction with users, stakeholders and policymakers. Reconciling climate science with decision-makers is precisely the aim of climate services (Buontempo et al., 2014). While national climate services spread worldwide, the extensive use of climate information is still very limited and some gaps in the information flow (e.g. an informative categorizing of types of users) often remain (Skelton et al., 2019). In light of this situation, the Swiss National Centre for Climate Services (NCCS, https://www.nccs.admin.ch) coordinated the new climate change scenarios for Switzerland (CH2018, 2018), https://www.climate-scenarios.ch), which aim to improve upon its predecessor (CH2011, 2011) in terms of providing user-oriented information (e.g. through user-tailored brochures) and scientific content (e.g. quantitative information on extremes and transient datasets) (Skelton et al., 2019). CH2018 made use of the largest collection of state-of-the-art regional climate model ensemble from the EURO-CORDEX initiative (Jacob et al. 2014, Kotlarski et al. 2014) to produce probabilistic climate projections at different spatial scales (as regional means, on a 2 km grid and at localized stations) for a large set of variables and climate indices. Among others, also future changes of heat stress conditions were analyzed for 83 Swiss locations (CH2018, 2018).

The aim of the present work is to refine and further tailor the

CH2018-based projections of heat stress and to make them more useable to users. First, we characterize projected changes of heat stress (single-day events and heat stress spells) and, secondly, we use climate analogs, based on the frequency and duration of heat stress spells, to interpret and ease the dissemination of the climate change information. A climate analog is defined as a place with a recent past climate similar to the values expected at the place of interest in the future (Ford et al. 2010, Dahinden et al. 2017, Matthews et al. 2017), in this case, with respect to heat stress spells. Analog methodologies can provide a first approximation of opportunities and limitations when coping with climate change and have a great potential in vulnerability research (Glantz 1991, Ford et al. 2010). At an individual level, the association of future heat stress with past events across scales and places allows to connect future changes with personal experience.

The paper is structured as follows: Data, methods and characterization of different indices are described in Section 3, Results (Section 4) comprise the evaluation of the methodology, the estimation of projected changes and identification of climate analogs and the main conclusions can be found in Section 5.

Material and methods

Heat stress index

A large number of heat stress indices exist that attempt to express environmental heat exposure by one single value (see e.g. Blazejczyk et al. 2012, Coccolo et al. 2016 for a review). A frequently applied index that is also used in the present work is the Wet Bulb Temperature TW (Sherwood and Huber 2010, Pal and Eltahir 2016). TW represents the temperature of an air parcel if cooled at constant pressure until saturation by the evaporation of water into it; at 100% relative humidity it equals the air (dry bulb) temperature. TW can be measured by covering a standard thermometer bulb with a wet cloth and ensuring full ventilation. Unlike more complex heat stress indices, such as the Wet Bulb Globe Temperature (Lemke and Kjellstrom, 2012) or the Universal Thermal Climate Index (Langner et al., 2014), TW can be easily derived from temperature and humidity measurements alone by means of thermodynamic equations (Davies-Jones, 2008) or, as in this work, by the empirical formula derived by Stull (2011), using air temperature and relative humidity, as implemented in the R package *HeatStress* (Casanueva, 2019a).

It is well known that heat stress and heat exposure vary throughout the day, and hence its impacts, for instance in terms of labour productivity (Kjellstrom et al., 2009). Sub-daily meteorological variables are, however, not readily available for most of the climate model simulations. Bearing this in mind, a sensitivity analysis to the use of daily aggregated data (i.e. daily minimum, maximum or mean quantities) of the input variables (air temperature and relative humidity) was carried out to find the best approximation of the daily maximum TW that would be associated with maximum heat stress. The analysis was based on station observations that are available at hourly resolution and which were aggregated to daily values to mimic climate model data at daily resolution. Several combinations of temperature and humidity were considered (e.g. daily mean temperature and relative humidity, daily maximum temperature and minimum relative humidity, etc.) and compared to the maximum TW obtained from hourly data (Fig. A1 in the Supplementary Material). The best approximation consisted of using daily maximum temperature and relative humidity calculated from daily maximum temperature and daily mean specific humidity (with low variability along the day). The latter combination approximately mimics daily minimum relative humidity which is often present at the time of maximum temperature, i.e. at the time of maximum heat stress, but not available from model data. Thus, the input variables needed from observations and climate simulations were daily maximum temperature and daily mean specific humidity.

The highest TW values recorded on Earth are close to 35 °C, which is the theoretical limit of survivability for a fit human being (Sherwood and Huber 2010, Buzan et al. 2015, Pal and Eltahir 2016). A TW of 35 °C greatly reduces the possibility of evaporation at skin level to cool the body, since the skin (usually at 35 °C or below) must be cooler than the body core (around 37 °C) for metabolic heat to be conducted to it. According to Vecellio et al. 2022, the 35 °C threshold overestimates real-world conditions and controlled experiments showed that critical wet-bulb temperatures are 25–28 °C in hot-dry environments and 30–31 °C in warm-humid environments. In addition, lower thresholds may also have other impacts on human beings. For instance, the safe working time greatly decreases for people performing heavy work when the wet bulb temperature is >30.8 °C (Liang et al., 2011). Those thresholds are rarely reached in Switzerland, where the highest ever recorded values reached 22–25.5 °C in low-lying stations. Furthermore, a TW threshold of 22 °C would trigger the same amount of (level 3) heat warnings based on the heat index (Burgstall et al., 2019).

Building upon CH2018, three heat-stress-derived indices (based on daily maximum values of TW) were considered to describe **single-day heat stress**: summer mean (TWmean) and maximum TW (TWx), and the number of summer days with TW above 22 °C (TWg22), which accounts for intense heat stress. Additionally, we characterized **heat stress spells** as events with TW above 22 °C for at least three consecutive days, which would roughly mimic heat warnings of level 3 "yellow" (out of 4 levels). We analyzed both the heat spells frequency (number of events per year, HSF) and duration (median length of all the individual events lasting 3 or more days, HSD, see Table 1).

Observational data

The observational reference considered in this work consists of the automatic monitoring network provided and maintained by MeteoSwiss (SwissMetNet[1], SMN). We used a set of 83 stations with at least 83% of data in the period 1981–2010 (i.e. 25 out of the 30 years; Fig. 2a) for the variables of interest, namely daily maximum air temperature and daily mean specific humidity. Note that directly measured variables are air temperature, relative humidity and air pressure at station level and, thus, specific humidity is derived from air pressure and vapour pressure (the latter obtained from air temperature and relative humidity). Due to the high amount of missing data in surface air pressure in many stations, missing values were replaced by 1013.25 hPa, for which the TW Stull equation holds. Hourly values of air temperature and relative humidity were further considered for the sensitivity analysis described in Sect. 3.1 (Fig. A1 in the Supplementary Material).

Model data and bias correction

Regional climate model (RCM) simulations from the CORDEX initiative (Coordinated Regional Downscaling Experiment; Giorgi et al.

Table 1
Definition of the heat stress indices used in this work.

Code	Definition	Units
TWmean	Summer mean TW	°C
TWx	Summer maximum TW	°C
TWg22	Number of summer days with TW > 22 °C	days
HSF	Heat spells frequency: number of heat stress spells per year (a heat spell occurs when TW > 22 °C for at least 3 consecutive days)	–
HSD	Heat spells duration: median length of all heat stress spells in a 30-year period (a heat spell occurs when TW > 22 °C for at least 3 consecutive days)	days

[1] https://www.meteoswiss.admin.ch/weather/measurement-systems/land-based-stations/automatic-measurement-network.html

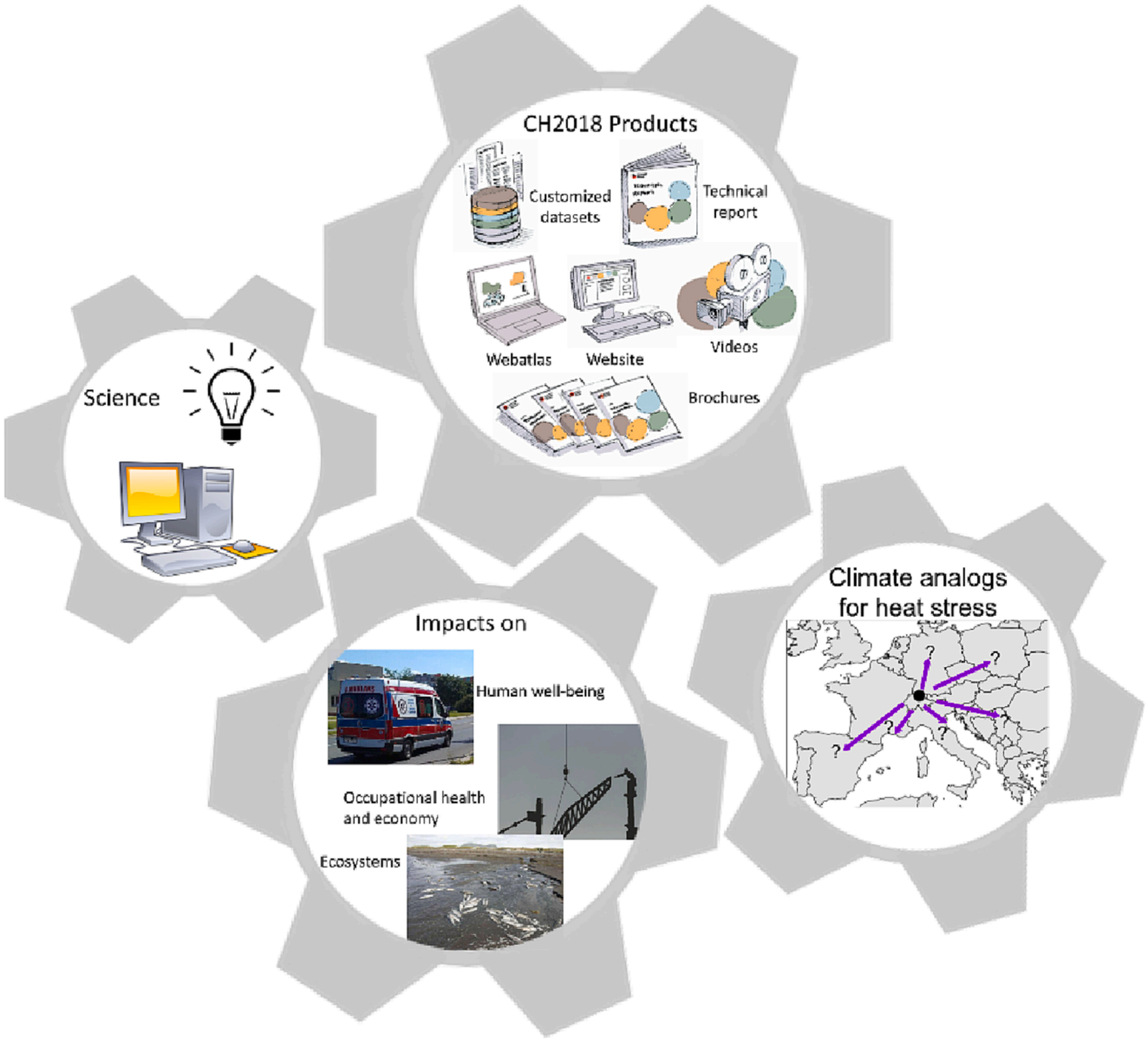

Fig. 1. Framework of the present study, which builds upon the CH2018 scenarios (scribbles for the products were designed by zeichenfabrik.ch) and extends to climate analogs for heat stress. (Other illustrations and photos are licensed under Creative Commons Zero, Public Domain Dedication).

2008; Jones 2010; Jacob et al. 2014; Kotlarski et al. 2014) were considered to derive CH2018 climate change projections. The model simulations (hereafter GCM-RCM chains) were performed by 6 RCMs driven by 9 different global climate models (GCMs), at two horizontal resolutions (0.11° and 0.44°, approximately 12 and 50 km) and covering three Representative Concentration Pathways (RCP 2.6, RCP 4.5 and RCP 8.5), which added up to 67 chains (see Table A1 in the Supplementary Material). These simulations are accessible via the Earth System Grid Federation (ESGF, https://esgf.llnl.gov/, extracted in May 2017). Herein, transient projections of TW from 1981 until 2099 were obtained from daily maximum temperature and daily mean specific humidity data at the closest grid boxes to the SMN stations (Sect. 3.2) for each GCM-RCM chain. The reader is referred to Sørland et al., 2020 for more details on the construction of the CH2018 multi-model ensemble, including the description of a time-shift-based pattern scaling approach using global mean surface temperature of the driving GCM as control parameter (Herger et al., 2015). The latter aided to obtain an equal number of simulations for each scenario to ensure comparability. The ensemble finally consisted of 20 GCM-RCM chains for RCP 2.6, RCP 4.5 and RCP 8.5 (green cells in Table A1 in the Supplementary Material).

Regional climate models are prone to systematic biases and, despite the increased spatial resolution of the EURO-CORDEX RCMs, they cannot represent local processes at finer scales than the grid spacing. Empirical quantile mapping (QM, Déqué, 2007) was used as downscaling and bias correction method in CH2018 to overcome these two limitations and bridge the gap between the regional and local scales. The reader is referred to CH2018, 2018, Feigenwinter et al., 2018 and Kotlarski 2019 for details on the QM implementation.

QM is a univariate bias correction method and in this work it was applied independently to the daily maximum temperature and daily mean specific humidity as simulated by the underlying EURO-CORDEX RCMs. The TW is then calculated from the two bias-corrected components, using the constant value of surface air pressure of 1013.25 hPa. Herein, QM was calibrated between the EURO-CORDEX RCMs and the SMN observations in the reference period 1981–2010. The correction functions were then applied transiently for the period 1981–2099. Note that years 2006–2010 from the projections were merged with the historical runs to complete the calibration period. Some of the results are

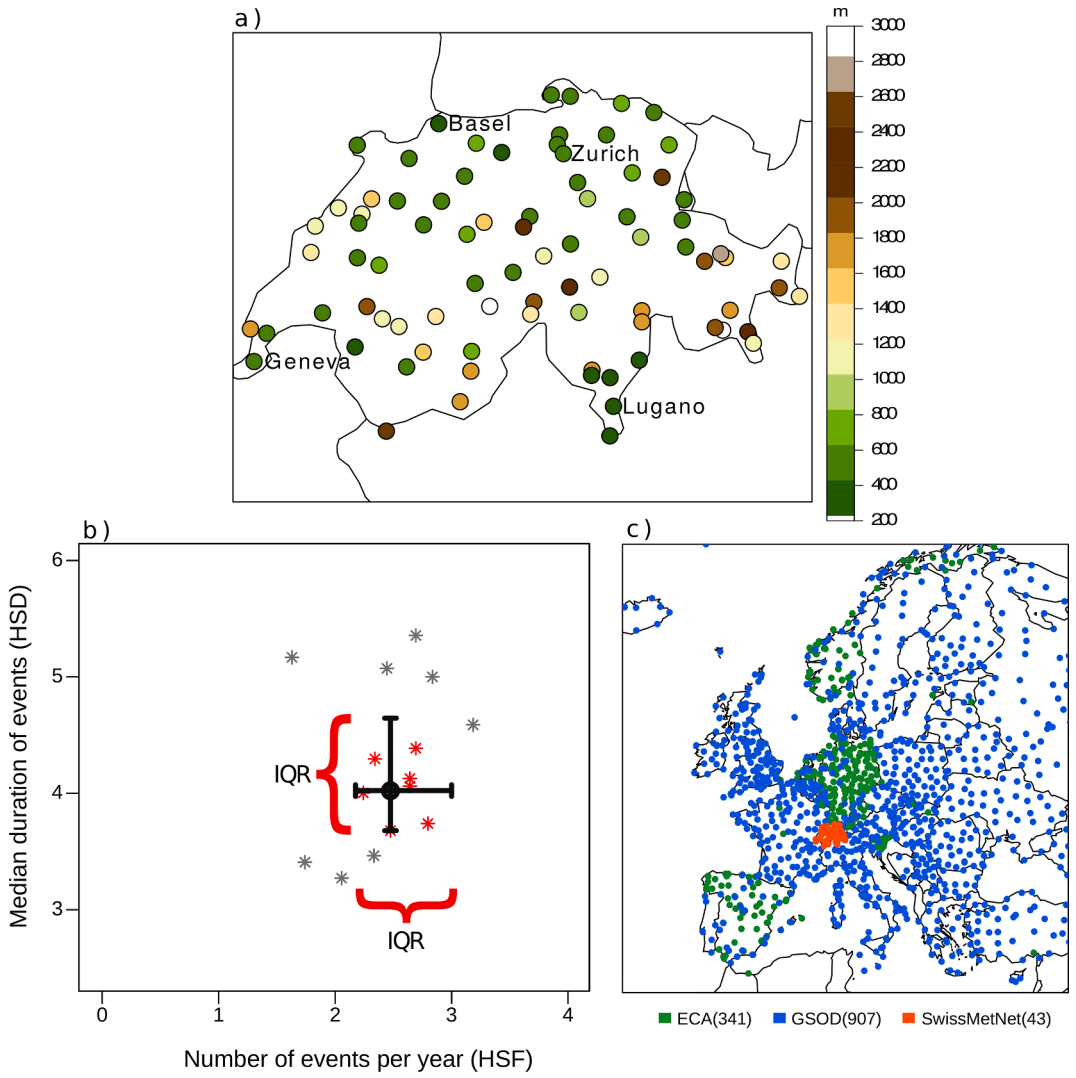

Fig. 2. (a) Set of 83 Swiss stations for which heat stress is assessed (four labeled stations are used in subsequent analyses). Colors depict the stations' elevation. (b) Illustrative diagram for the identification of climate analogs based on heat spells. The central point represents the multi-model median projected value of frequency (X-axis) and duration (Y-axis) of events at a target location (2.5 events/year and median length of 4 days in the example) and the whiskers represent the interquartile range (IQR) of the model ensemble. The grey stars are the potential analogs; those within the range of the model ensemble IQR are considered good analogs (red stars). (c) Reference station set for the analogs identification, from three different data sources (colors; see text). (For interpretation of the references to colour in this figure legend, the reader is referred to the web version of this article.)

presented for specific 30-year time slices for near-term (2020–2049), mid-term (2045–2074) and long-term projections (2070–2099), compared to the reference period (1981–2010). In the following, we simply refer to them by their central years, i.e. 1995, 2035, 2060 and 2085, respectively.

Climate analogs

The impacts of climate change primarily manifest themselves at regional and local scales. Therefore, regional- or country-specific analyses are required to inform decision makers. One straightforward approach to interpret and communicate changes in climate at smaller spatial scales is by means of climate analogs (Ford et al. 2010, Dahinden et al. 2017 and references therein). This method consists of identifying a place with a recent past climate similar to the projections of the place of interest. The methodology has been applied to global climate models for temperature and precipitation (Dahinden et al., 2017) and heat stress analogs (Matthews et al., 2017). For instance, with 1.5 °C global warming, Lagos (Nigeria) might experience heat stress levels similar to Delhi (India) during the recent past reference climate (1979–2005) and the closest analog for the climate of Shanghai (China) would be today's climate of Karachi (Pakistan) (Matthews et al., 2017). Climate analogs were also assessed within CH2018, showing e.g. that the best temperature analogs for Swiss locations at increased future warming levels are found in southern European locations (CH2018, 2018). Some web tools[2,3] have been similarly developed to find climate analogs or "climate twins" for representative cities worldwide and in North America building upon Bastin et al. 2019, Fitzpatrick and Dunn 2019.

Different criteria can be used to identify climate analogs, for instance, mean quantities such as the mean annual cycle of temperature and precipitation (Dahinden et al. 2017, CH2018, 2018) or frequency of heat index above a specific threshold (Matthews et al., 2017). Here we identify climate analogs based on the frequency and duration of heat stress spells (see Sect. 3.1). Similarity was assessed by means of the Euclidean distance between the multi-model median projected value of HSD and HSF at the Swiss target location and the observed counterparts

[2] https://fitzlab.shinyapps.io/cityapp/.
[3] https://hooge104.shinyapps.io/future_cities_app/.

(see illustrative diagram in Fig. 2b). The reference dataset for the analogs' identification consisted of a large set of European stations (approximately 1300 stations, see Fig. 2c), which resulted from a combination of the ECA&D (European Climate Assessment & Dataset; Klein Tank et al. 2002) dataset, the GSOD dataset (Global Surface Summary of the Day; Smith et al. 2011) and SMN data set (Sect.3.1) in Switzerland. These data were also the observational reference for European-scale climate change projections of heat stress derived by Casanueva et al. 2020. Selected ("good") analogs were those European locations which lay within the interquartile range of the full model ensemble (i.e. within 50% of the models), of both HSD and HSF (Fig. 2b), i.e. the criterion is defined in a bi-variate way.

Results

Evaluation of the bias correction method

In a multivariate context, bias correction is typically done by adjusting the input variables independently prior to the index calculation (see, e.g. Yang et al. 2015). This approach might lead to inconsistencies in spatio-temporal fields and in inter-variable relationships (Ehret et al., 2012), and more sophisticated multivariate bias-correction methods have been introduced (Vrac and Friederichs, 2015). However, Wilcke et al. 2013 showed that the inter-variable dependencies as represented by raw RCM data are approximately preserved by QM and are not strongly distorted. Furthermore, according to Casanueva et al. (2019) the adjustment of the individual distributions of temperature and humidity implicitly leads to a better representation of the joint distribution of heat stress (wet bulb globe temperature in the cited work). Here the QM performance in a multivariate context is evaluated by comparing the observed and simulated TW distribution for the reference period 1981–2010. Although no cross validation has been applied (the same period, 1981–2010, is used for calibration and validation), this evaluation can be considered fair, since TW is not directly targeted in the calibration of the QM but is derived from two independently corrected variables (daily maximum temperature and daily mean specific humidity). Fig. 3 shows quantile–quantile plots with the observed and simulated quantiles of TW before (black; i.e. raw RCM data) and after the bias correction by QM (blue) of the input variables, for a set of example Swiss locations and for one example climate model chain. Large biases are found for the raw data, especially for the cases for which the elevations of the model grid box and the station are very different (note that no height correction has been applied to the raw data). The correction of the two independent variables leads to a good representation of the TW in the historical period. Similar conclusions hold for other GCM-RCM chains.

Climate change projections of single-day heat stress

Observed values of summer mean (TWmean) and maximum (TWx) wet bulb temperature in Switzerland are largest in Canton Ticino in the Southern part of Switzerland, where they amount to 18–19 °C and 22–24 °C, respectively (Fig. 4, first row). High values of TWx are also found at most of the non-mountainous stations (e.g. Basel, Geneva, Zurich). The threshold of 22 °C is, on average, only exceeded in a few locations. This threshold approximately corresponds to the observed summer 98th percentile of TW in Zurich and Geneva and the 92nd percentile in Lugano in the reference period. The largest frequencies are found in the low-lying stations in Ticino (7 days in Lugano and 12 in Magadino/Cadenazzo and Stabio).

At all stations the three TW-derived indices are projected to gradually increase until the end of the century (Fig. 4). For RCP 8.5, the maximum wet bulb temperature TWx increases by 1 to 2 °C, 2 to 3.5 °C, and 3 to 4.5 °C (multi-model median, depending upon the station) in the three future periods, respectively. In Lugano, for instance, summer mean and maximum TW are projected to reach 21–23 °C and 25–27 °C (multi-model range), respectively, by 2085. Heat stress extremes, unlike temperature extremes themselves, show an increase in the upper tail of the distribution similar to the increase in the mean. This absence of amplification of the climate-change signal in the extreme tail of the distribution may be caused by the role of humidity, since the slight decrease in relative humidity (CH2018, 2018, Brouillet and Joussaume 2019) might counteract the larger increase in extreme temperatures.

The projected number of summer days with TW > 22 °C (TWg22)

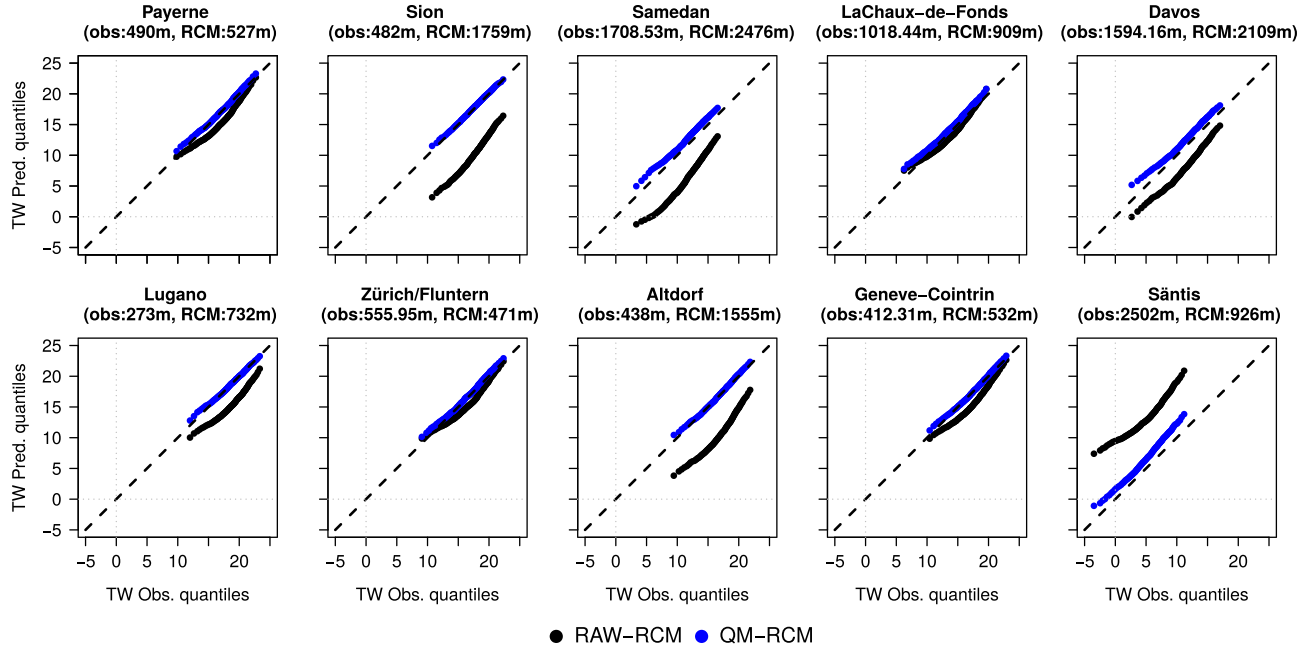

Fig. 3. Quantile-quantile plot showing the quantiles of the observed and simulated summer TW from the uncorrected data (black, "RAW-RCM") and corrected data (blue, "QM-RCM") for ten representative stations in Switzerland. The RCM data correspond to the closest grid box to the stations from the simulation MPI-M-MPI-ESM-LR CLMcom-CCLM4-8–17 at 0.11° and the reference period (1981–2010). The altitudes of the station and the corresponding grid box are given in brackets. (For interpretation of the references to colour in this figure legend, the reader is referred to the web version of this article.)

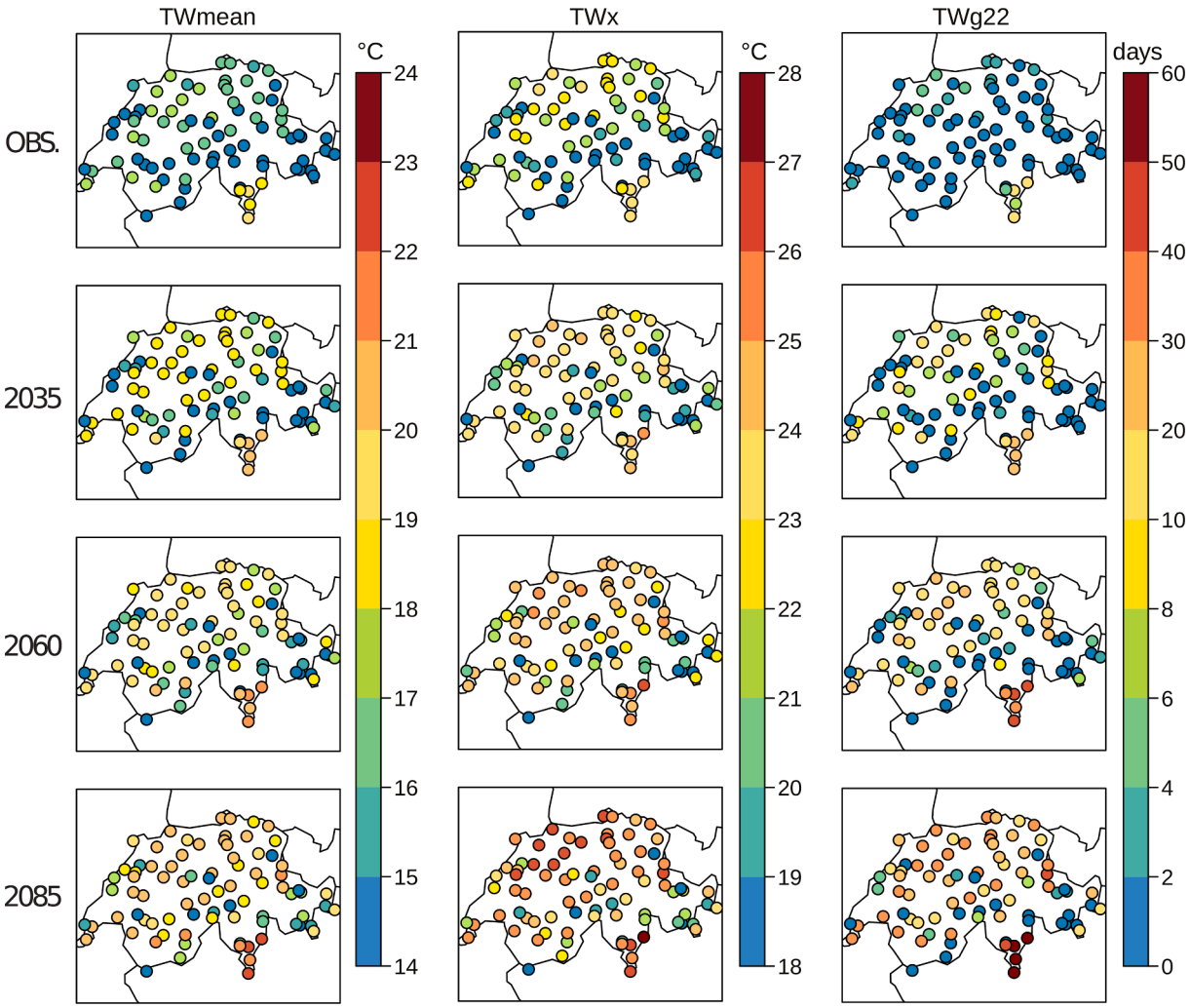

Fig. 4. Observed values (first row, period 1981–2010) and climate-change projections (2nd–4th rows) for summer mean (TWmean) and maximum TW (TWx), and the number of days with TW > 22 °C (TWg22) displaying the multi-model median after bias-correction (20 simulations, see Sect. 3.3) for the three 30-year future periods ("2035" for 2020–2049, "2060" for 2045–2074 and "2085" for 2070–2099) and according to the RCP 8.5 scenario.

implies that, on average, more than one-third of summer days will feature severe heat-stress conditions in many locations of the Swiss Plateau (Zurich, Basel, Geneva) and in inner-alpine Alpine valleys (Sion, Interlaken, Chur). The canton of Ticino in the South is the region with the largest increases in TWg22, with increases of up to 15, 30, and 45 days in the three future periods, respectively. At mountainous stations, TWg22 only slightly increases or does not change, since the threshold of 22 °C is hardly ever exceeded even in a warmer future climate (0–2 days). These results for TWg22 are qualitatively consistent with the projections of summer days in Switzerland (CH2018, 2018).

Transient projections for summer maximum wet bulb temperature in four example stations under RCP 8.5 (Fig. 5) show a continuous increase until the end of the century and model uncertainty of about 3 to 4 °C. In Zurich and Geneva the threshold of 22 °C was only exceeded in extreme summers (e.g., 2003, 2010; black lines) in the past, but projected values at these locations are well above that threshold from mid-century onward. That implies that these four locations will experience elevated heat stress conditions at least once every summer. Large interannual variability remains in the future, as represented by an example simulation depicted with a blue line.

Results for RCP 2.6 and RCP 4.5 (Figs. A2 and A3 in the Supplementary Material) indicate similar regional patterns to RCP 8.5 until mid-century, also with the largest increases of heat stress in Canton Ticino and at stations in the lowlands. For RCP 2.6, the projected values for the late 21st century scarcely differ from the mid-century values, reaching 19–20 °C and 23–24 °C for mean and maximum TW in Lugano, respectively. Summer mean and maximum TW are projected to reach 20–21 °C and 24–25 °C by 2085 for RCP 4.5. TWg22 differs substantially between RCP 2.6 and RCP 8.5 in magnitude and spatial extent, with such conditions occurring about 3 to 5 times more frequently for RCP 8.5. Specifically, differences between RCP 2.6 and RCP 8.5 in projected TWg22 are depicted in Fig. 6, including multi-model uncertainty, for the four example stations. A considerable increase of TWg22 is evident by 2035 compared to the reference period regardless of the emission scenario. Whereas projected TWg22 remains similar over time under RCP 2.6, a large increase is projected under RCP 8.5 by 2085 at the four stations accompanied with a widening of the uncertainty range. One third (half) of summer days might experience intense heat stress in Basel, Zurich and Geneva (Lugano) under the strong emission scenario in an average summer by 2085.

Future extension of the heat stress season

Previous results show the increase of heat stress (mean, maximum and exceedance of the 22 °C threshold) for the standard summer season, i.e. from June to August (JJA). However, in a climate change context, summers are projected to be longer lasting in the Northern Hemisphere as a consequence of global warming (Lin and Wang et al. 2022). During

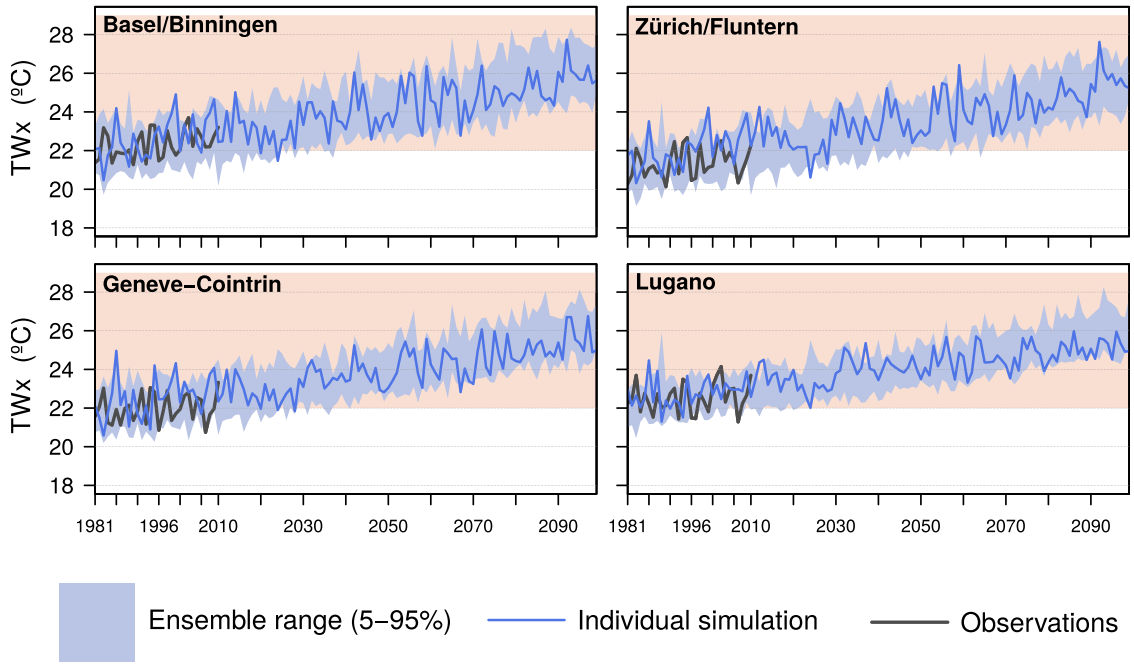

Fig. 5. Temporal evolution of the summer maximum wet bulb temperature (TWx, °C) at four Swiss stations for RCP 8.5. In this figure, the maximum value for each summer is obtained from the daily TW values smoothed with a 3-day moving average. Observed values are depicted by the black line, the blue shading indicates 90% of the multi-model range (20 simulations, see Sect. 3.3), and the blue line shows an individual simulation (MPI-M-MPI-ESM-LR CLMcom-CCLM4-8–17 at 0.11°) to illustrate historical and future interannual variability (particularly in these examples this simulation is, on average, close to the multi-model ensemble median by the end of the century). The light red band depicts TW values above the 22 °C threshold. (For interpretation of the references to colour in this figure legend, the reader is referred to the web version of this article.)

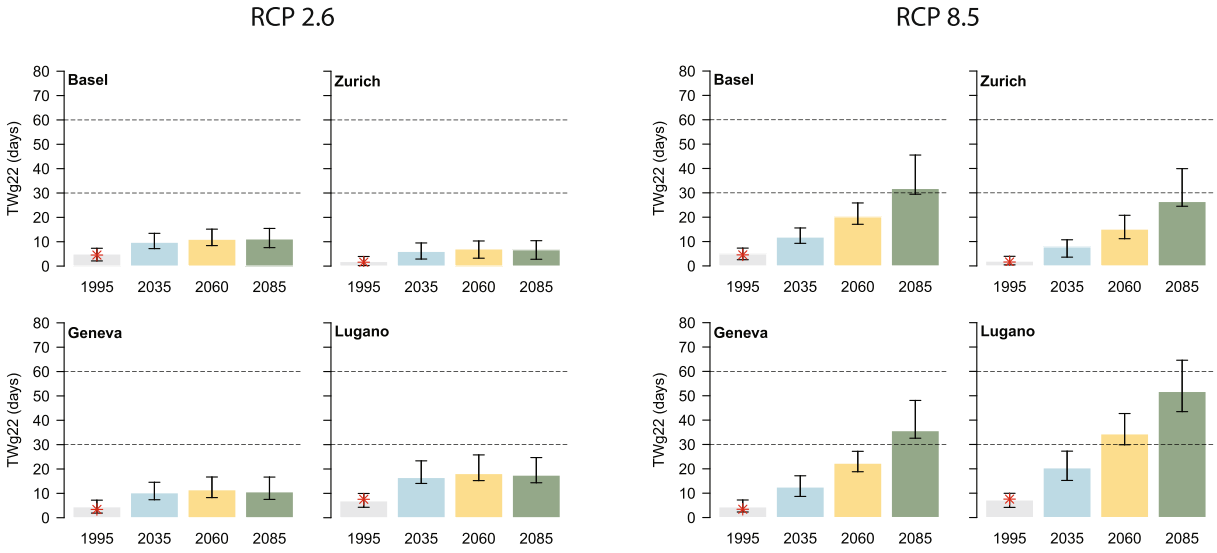

Fig. 6. Observed (red stars) and simulated (bars) values of TWg22 for RCP 2.6 (left) and RCP 8.5 (right) at four example stations. Values are multi-year means over 30-year periods centered in 1995 (1981–2010), 2035 (2020–2049), 2060 (2045–2074) and 2085 (2070–2099). The grey (colored) bars depict results for the historical (future) bias-corrected simulations. The height of the bars represents the multi-model ensemble median and the whiskers indicate the 5–95% model range (pattern-scaled data, i.e. 20 simulations for both RCPs, see Sect. 3.3). Results for RCP 4.5 are found in the Supplementary Material (Fig. A4). (For interpretation of the references to colour in this figure legend, the reader is referred to the web version of this article.)

1952–2011, summer length extended at an average rate of 4.2 days every 10 years in the Northern Hemisphere (Wang et al. 2021). By the end of the 21st century, summers might last around one month more for a medium emission scenario and up to two months more for the strongest emission scenario relative to 1961–2014, on average, in the Northern Hemisphere (Lin and Wang, 2022).

Bearing all the above in mind, we estimated the increase in TWg22 when May and September are additionally considered (Fig. A5 in the Supplementary Material). We found that Canton Ticino might reach TW above 22 °C beyond JJA by mid-century (up to 2 days more for RCP 4.5 and 5 days more for RCP 8.5, values represent multi-model ensemble median) and can rise by 5 to 7 days by 2085 for RCP 8.5, with the highest values reached in Magadino and Grono with increases of approximately 8 and 12 days, respectively. The threshold might be also surpassed in

May and September in some other lowland stations of Switzerland by the end of the century and RCP8.5 (3–5 more days depending on the station). The annual cycle of TWg22 reveals that, under RCP 8.5 (Fig. 7), the threshold may be easily exceeded in September by the end of the century in lowland stations and from mid-century onwards in Ticino. Multi-model spread can be quite large for peak months (around 6 to 7 days in July) and similar or slightly smaller for September. Still, multi-model ensemble median values for September are slightly above observed values in July, when maximum values occur. Under RCP 2.6 (Fig. A6 in the Supplementary Material), very few exceedances occur beyond JJA and the annual cycle suffers little variations from 2060 to 2085. Some days with TW above 22 °C might occur in September in Ticino either by 2060 or 2085 under RCP 4.5, where the multi-model spread overlaps to a large extent (Fig. A7 in the Supplementary Material).

In the following, full years are considered for the calculation of heat stress spells, to account for the future extension of the summer season and avoid cutting spells off.

Projected heat stress spells

Climate projections of heat stress spells (three or more days with TW $>$ 22 °C) are analyzed in terms of the frequency (HSF) and duration (HSD) of the events. Results for HSF (Fig. 8, upper panel) are aligned with those for TWg22 (Sect.4.2), with a pronounced increase towards the end of the century under RCP 8.5. The number of events might amount, on average, to 4–6 events per year under RCP 8.5 by 2085 in the four locations, which is about five times more than by 1995. This could be even worse for specific years. The increase is especially relevant for Basel and Geneva, where there is less than 1 event in present climate, on average. Under RCP 2.6, up to 2 events are projected in Basel and Geneva and up to 3.5 events in Lugano by the end of the 21st century. Despite the lower number of projected events under RCP 2.6, this represents an approximate doubling of the average frequency in present climate.

The duration of the heat stress spells (Fig. 8, lower panel) ranges between three and four days in present climate at all four stations. HSD is projected to only slightly change under RCP 2.6, with no change (Basel and Geneva) or a maximum increase of 1 day (Zurich and Lugano), according to the multi-model median. The uncertainty range might imply ± 1 day in Basel, Geneva and Lugano by the end of the century, whereas a larger uncertainty is found for Zurich (up to 6 days). Under RCP 8.5, HSD might increase by one (Basel and Geneva) or two (Zurich and Lugano) days by 2085, according to the multi-model median. These results represent a duration of approximately 4–6 days in Basel, Zurich and Geneva and 6–8 days in Lugano by the end of the century. Modeled HSD and HSF show good agreement with the observed counterparts in the historical period (see grey bars and red stars in Fig. 8), except for

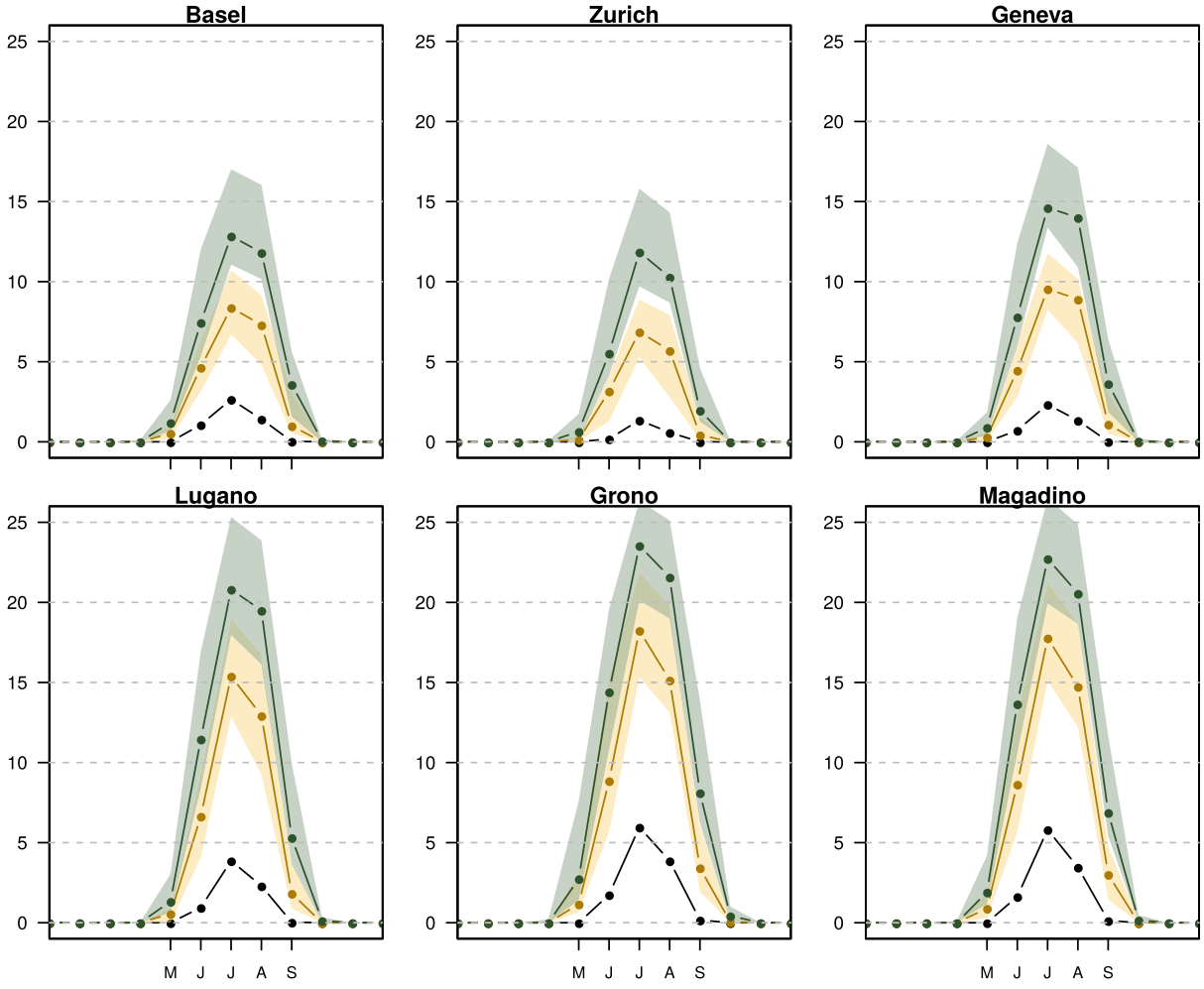

Fig. 7. Annual cycle of TWg22 (days) in six example stations (three stations in the second row are in Canton Ticino). Black lines depict the observations and coloured bands illustrate future conditions (yellow for 2045–2074, green for 2070–2099) under RCP 8.5 (shading indicates 5–95% model range and lines multi-model ensemble median). Results for RCP 2.6 and RCP 4.5 can be found in the Supplementary Material (Figs. A6, A7). (For interpretation of the references to colour in this figure legend, the reader is referred to the web version of this article.)

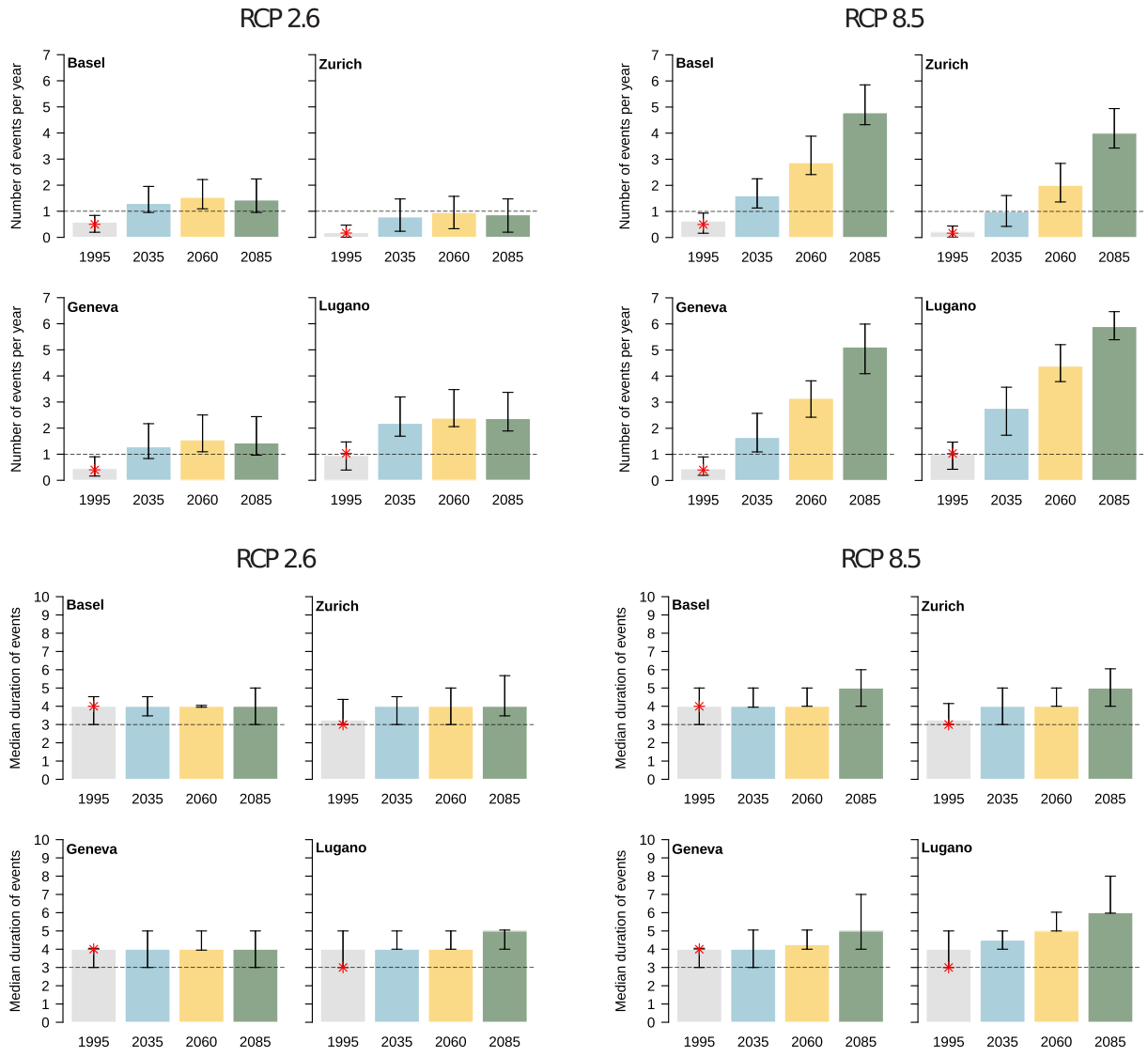

Fig. 8. As Fig. 6, but for the frequency (HSF, upper panels) and duration of heat stress spells (HSD, lower panels). Results for RCP 4.5 are found in the Supplementary Material (Fig. A4).

HSD in Lugano which is slightly overestimated by most models.

Climate analogs based on heat stress

We use climate analogs to provide a first approximation of places with a recent past climate similar to the future projections at the Swiss target stations in terms of number and duration of heat stress spells (Sect. 3.4). The locations of the analogs largely depend on the emission scenario (Fig. 9), but a distinct spatial pattern becomes apparent. Analogs under RCP 2.6 are found in Central Europe (with best analogs for Basel, Geneva and Lugano along the French coast -e.g. in Bordeaux and Montpellier areas-, eastern Hungary or the Black Sea, c.f. Fig. A8 in the Supplementary Material), whereas analogs under RCP 8.5 are markedly shifted southwards, mainly found in southeastern Spain (e.g. Alicante, Murcia) and Italy (e.g. in Veneto and Puglia regions and Sicily). Geneva and Lugano present the southernmost analogs, aligned with the largest values of TWg22 (Fig. 6) and HSF and HSD (Fig. 8). The degree of similarity comprises the agreement in terms of the two components of the heat stress spells (HSF and HSD, see Sect. 3.4). Thus, the analogs' quality relies on specific criteria, here the robustness of the projections for the given indices. HSD presents larger multi-model uncertainty than HSF, especially in Zurich, Geneva and Lugano for RCP 8.5 (Fig. A8 in the Supplementary Material). Despite this, the distribution of good analogs (Fig. 9) is coherent with hotter and more humid places.

Although the identification of climate analogs is simply done considering climatological statistics and does not involve physical mechanisms or atmospheric flows, TW includes the combination of two variables (air temperature and relative humidity) which might have some advantages with respect to temperature alone. For illustrative purposes, heat spells are defined as three or more consecutive days with daily maximum temperature above 33 °C (MeteoSwiss, 2021), i.e. leaving out the effect of humidity. The duration and frequency of such events are obtained similarly to the previous HSD and HSF. While the meridional gradient of the climate analogs under the two RCPs is still noticeable, the uncertainty (interquartile range of the multi-model ensemble) is larger for heat spells based on temperature (Fig. A9 in the Supplementary Material), leading to larger uncertainty in the localization of good analogs (Fig. 10) since many more stations lie within the good analogs range. The uncertainty is so large that in some cases good analogs under RCP 2.6 are located further south than under RCP 8.5 (e.g. Zurich or Geneva). Interestingly, unlike the similar TW-analogs found for Basel and Geneva, substantial differences between the two locations are noticeable when only maximum temperature is considered.

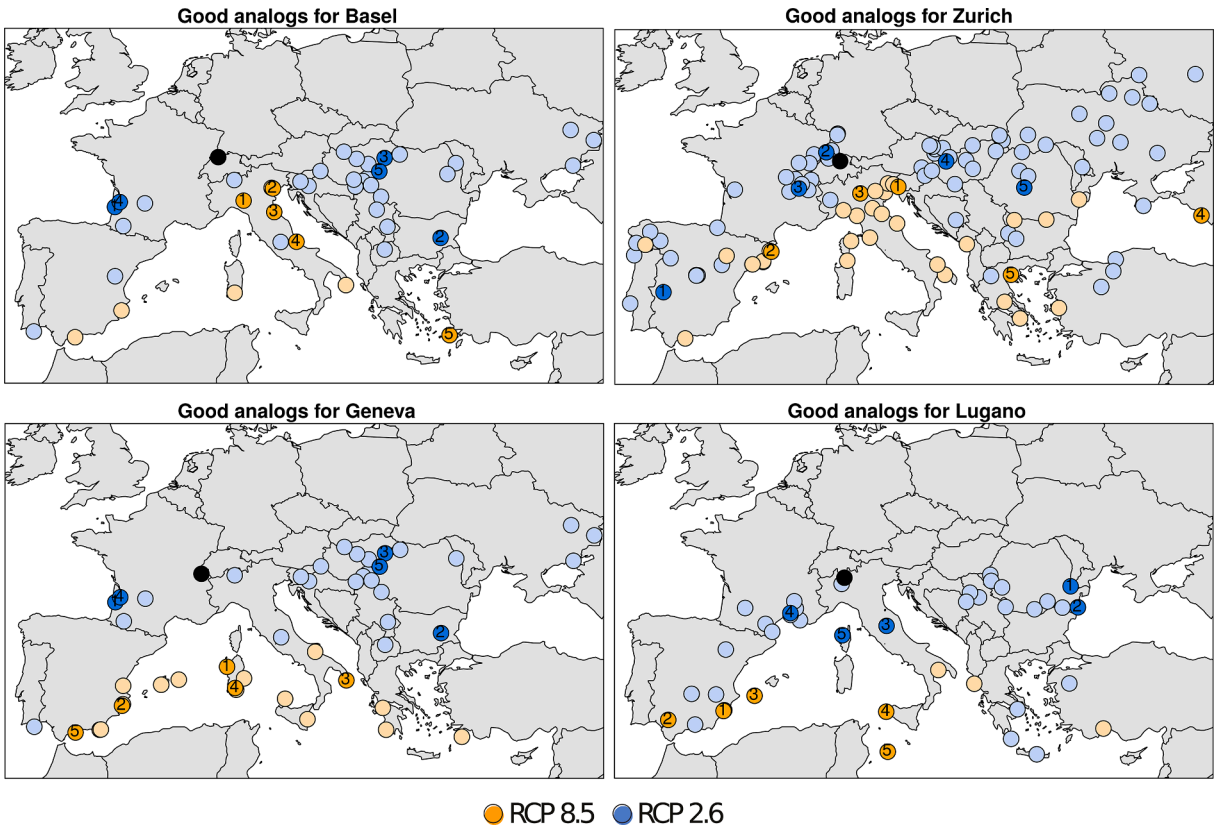

Fig. 9. Climate analogs based on heat stress spells for four example stations (Basel, Zurich, Geneva and Lugano, depicted in black in each panel) under RCP 2.6 (blue dots) and RCP 8.5 (orange dots) by 2070–2099. The best (closest) five analogs are marked from 1 to 5 (see more details in Fig. A8 in the Supplementary Material). Lighter colours represent further good analogs in the respective RCPs. See Sect. 3.4 for details in the analogs detection. (For interpretation of the references to colour in this figure legend, the reader is referred to the web version of this article.)

Note that here we present climate analogs in terms of heat stress (either temperature alone or based on TW), and that it is important to bear in mind that other aspects of climate, such as precipitation and seasonality, will differ between these analog locations. Other aspects of climate might change as climate changes in non-analogous ways or may be both non-analogous and also unchanging. Thus, users should be warned to avoid misinterpretations.

Summary and conclusions

The present work exploits and extends the CH2018 Swiss climate scenarios to evaluate the representation of heat stress conditions and to derive their future changes. For this purpose, we make use of relevant thresholds to characterize extreme heat conditions and to identify climate analogs. By doing so, we attempt to produce more applicable and more illustrative climate information which might foster the use and understanding of climate scenarios. Heat stress is expressed in terms of the wet bulb temperature and a set of derived metrics, considering single-day features and spells.

The results show a continuous increase of summer mean and maximum heat stress during the 21st century under the moderate (RCP 4.5) and strong (RCP 8.5) emission scenarios, which is accentuated towards the end of the century. High heat stress conditions (TWg22) are also projected to occur more often, with a 3–5 times stronger increase in terms of frequencies for the RCP 8.5 emission scenario compared to the RCP 2.6 mitigation scenario by the end of the 21st century. These results rely on the standard definition of summer (from June to August), but the heat stress season might potentially extend to neighbouring months in the future. This is particularly relevant in Canton Ticino from mid-century onwards under RCP 4.5 and RCP 8.5 and in other lowland stations by the end of the century for RCP 8.5, where we found that TWg22 in September could be slightly above observed values in July, when maximum values occur. These findings highlight the need to assess changes in extreme events beyond the typical definition of seasons, which can be especially relevant from an impacts and adaptation perspective.

Due to the cumulative effect of heat stress, the temporal sequence of days with intense heat stress is further assessed. The models represent the median duration and frequency of heat stress spells (events with TW above 22 °C for at least three days) fairly well in present climate, except for an overestimation of the duration in Lugano in the South of Switzerland. Under future climate change, the duration of the events changes only little but comes with a large model spread, whereas the frequency of heat stress spells shows more pronounced changes. The number of events might increase from 1 (or less) in present day climate to 4–6 events per year by the end of the century under RCP 8.5 in four representative low-lying cities. Despite a less accentuated increase under RCP 2.6, Basel, Geneva and Lugano might experience 2 to 3 events. Note that the selected stations are not located in city centers, but in their surroundings. It should therefore be assumed that heat stress is substantially higher within cities due to the urban heat island effect (Burgstall et al., 2021), which leads to an amplification of urban heat stress particularly pronounced during heatwaves (Fischer et al., 2012).

Climate analogs based on heat stress spells largely depend on the emission scenario considered. They can be found in Central Europe (with best analogs along the French coast or the Black Sea) under RCP 2.6 and they are markedly shifted southwards under RCP 8.5. This meridional shift should not be interpreted as a positive consequence of climate change, since even small changes can be detrimental to the health of elderly people and labour-intensive workers.

We acknowledge that climate analogs should be used with caution. Yet this methodology presents a first approximation to the identification

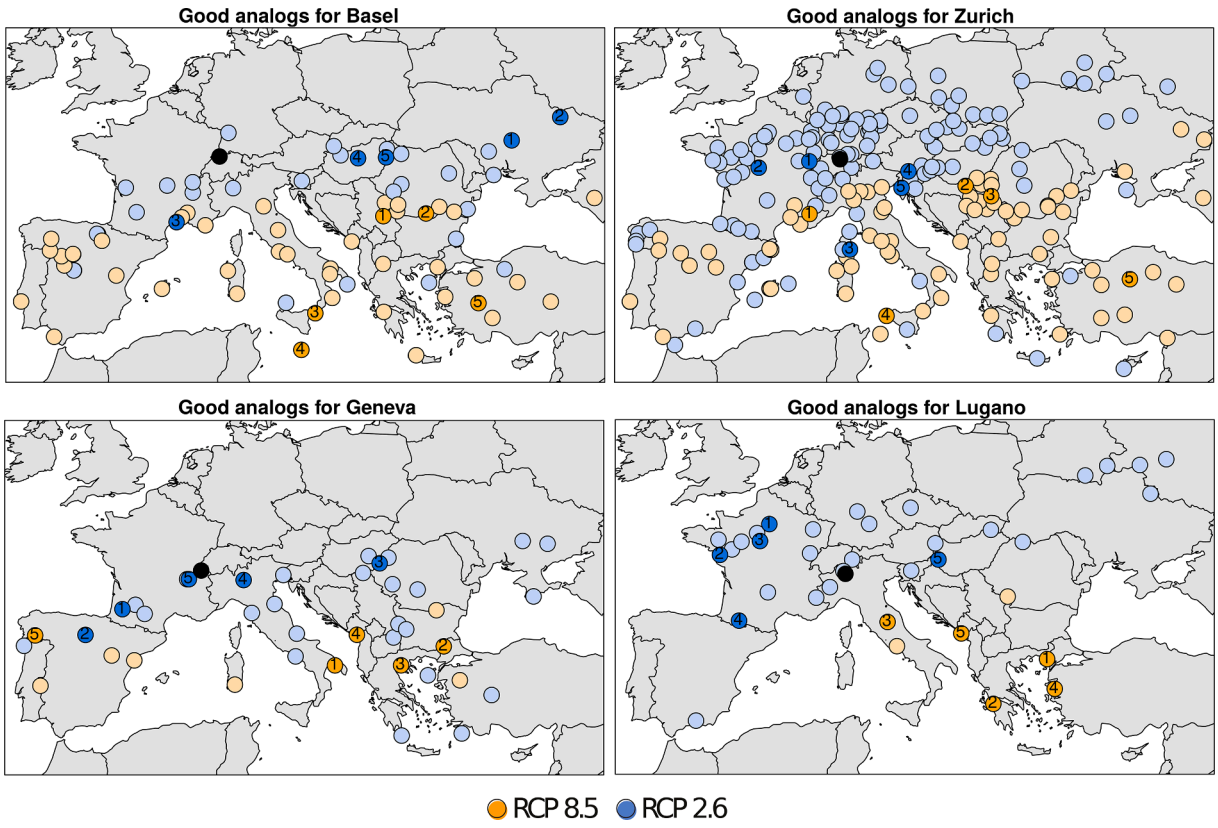

Fig. 10. As Fig. 9 But for heat spells defined as three or more consecutive days with maximum temperature above 33 °C by 2070–2099.

of similar climates and might help to recognize opportunities and limitations when coping with climate change (Glantz 1991, Ford et al. 2010). Despite the limitations, they can nevertheless be instrumental in the illustration and communication of future climates in a very intuitive way. In this work, climate analogs present two innovative aspects, 1) they are based on heat stress and 2) they are identified based on the duration and frequency of spells. Despite being a purely statistical approach, the first aspect allows to find analogs which are more feasible than temperature-only analogs from a thermo-physiological point of view. The second aspect emphasizes the cumulative feature of heat stress, which is especially relevant during early-summer heat waves for less acclimatized population (e.g. Central Europe). Furthermore, the comparison of heat stress indices with temperature indices reveals that the inclusion of humidity narrows down the localization of good analogs. This uncertainty reduction indicates that a multi-variate approach helps in characterizing the future climate using current measurements.

The projected increase of heat stress results in more frequent and extended occurrences of situations roughly connected to current heat warnings, thus highlighting the importance of timely and precise prevention strategies in the context of heat-health action plans. This work pursues the improvement of climate services by means of linking meteorological heat warnings to climate projections and producing more understandable climate projections through climate analogs.

CRediT authorship contribution statement

A. Casanueva: Formal analysis, Software, Visualization, Writing – original draft. **S. Kotlarski:** Conceptualization, Methodology, Software, Supervision, Writing – review & editing. **M.A. Liniger:** Conceptualization, Methodology, Supervision, Writing – review & editing, Funding acquisition. **C. Schwierz:** Conceptualization, Supervision, Writing – review & editing. **A.M. Fischer:** Conceptualization, Writing – review & editing, Funding acquisition, Project administration.

Declaration of Competing Interest

The authors declare that they have no known competing financial interests or personal relationships that could have appeared to influence the work reported in this paper.

Data availability

Data will be made available on request.

Acknowledgements

The authors are grateful to the World Climate Research Programme's Working Group on Regional Climate, and the Working Group on Coupled Modelling, former coordinating body of CORDEX and responsible panel for CMIP5. We also thank the climate modelling groups for producing and making available their model output, the Earth System Grid Federation infrastructure, an international effort led by the U.S. Department of Energy's Program for Climate Model Diagnosis and Intercomparison, the European Network for Earth System Modelling and other partners in the Global Organisation for Earth System Science Portals (GO-ESSP). We acknowledge the observational data providers: ECA&D project, the National Centers for Environmental Information, NESDIS, NOAA, U.S. Department of Commerce. We thank Curdin Spirig (ETH Zurich) and Dr. Jan Rajczak (MeteoSwiss) for pre-processing the simulation data. The authors are also grateful to Dr. Jan Rajczak for providing an earlier version of the quantile mapping code. We also thank the CH2018 group (www.climate-scenarios.ch) for technical support and scientific discussions and the Swiss National Supercomputing Centre (CSCS) for providing the technical infrastructure. We are also grateful to two anonymous reviewers for their constructive comments.

Financial support.

Financial support for this work is provided by the HEAT-SHIELD

Project (European Commission HORIZON 2020, research and innovation programme under the grant agreement 668786). A.C. acknowledges support from Project COMPOUND (TED2021-131334A-I00) funded by MCIN/AEI/10.13039/501100011033 and by the European Union NextGenerationEU/PRTR.

Appendix A. Supplementary data

Supplementary data to this article can be found online at https://doi.org/10.1016/j.cliser.2023.100372.

References

Bastin, J.-F., et al., 2019. Understanding climate change from a global analysis of city analogues. PLoS One 14, 1–13. https://doi.org/10.1371/journal.pone.0217592.

Blazejczyk, K., et al., 2012. Comparison of UTCI to selected thermal indices. Int. J. Biometeorol. 56, 515–535. https://doi.org/10.1007/s00484-011-0453-2.

Brouillet, A., Joussaume, S., 2019. Investigating the role of the relative humidity in the co-occurrence of temperature and heat stress extremes in CMIP5 projections. Geophys. Res. Lett. 41, 435–443. https://doi.org/10.1029/2019GL084156.

Buontempo, C., Hewitt, C.D., Doblas-Reyes, F.J., Dessai, S., 2014. Climate service development, delivery and use in Europe at monthly to inter-annual timescales. Clim. Risk Manag. 6, 1–5. https://doi.org/10.1016/j.crm.2014.10.002.

Burgstall, A., et al., 2021. Urban multi-model climate projections of intense heat in Switzerland. Clim. Serv. 22, 100228 https://doi.org/10.1016/j.cliser.2021.100228.

Burgstall, A., Casanueva, A., Kotlarski, S., Schwierz, C., 2019. Heat Warnings in Switzerland: reassessing the choice of the current heat stress index. Int. J. Env. Res. Public Health 16, 2684. https://doi.org/10.3390/ijerph16152684.

Buzan, J.R., Oleson, K., Huber, M., 2015. Implementation and comparison of a suite of heat stress metrics within the Community Land Model version 4.5. Geosci. Model Dev. 8, 151–170. https://doi.org/10.5194/gmd-8-151-2015.

Casanueva, A., et al., 2019. Climate projections of a multivariate heat stress index: the role of downscaling and bias correction. Geosci. Model Dev. 12, 3419–3438. https://doi.org/10.5194/gmd-12-3419-2019.

Casanueva, A., et al., 2020. Escalating environmental summer heat exposure-a future threat for the European workforce. Reg. Environ. Chang. 20, 40. https://doi.org/10.1007/s10113-020-01625-6.

Casanueva, A., 2019a. *anacv/HeatStress: zenodo (Version v1.0.7_zenodo). Zenodo. http://doi.org/10.5281/zenodo.3264929.*

CH2011, 2011. *Swiss climate change scenarios CH2011.* Zurich: C2SM, MeteoSwiss, ETH, NCCR Climate and OcCC, 88pp. ISBN: 978-3-033-03065-7.

CH2018, 2018. CH2018 – Climate Scenarios for Switzerland, Technical Report, Zurich: National Centre for Climate Services. 271pp. ISBN: 978-3-9525031-4-0.

Ciuha, U., et al., 2019. Interaction between indoor occupational heat stress and environmental temperature elevations during heat waves. Weather Clim. Soc. 11, 755–762. https://doi.org/10.1175/WCAS-D-19-0024.1.

Coccolo, S., Kämpf, J., Scartezzini, J.-L., Pearlmutter, D., 2016. Outdoor human comfort and thermal stress: A comprehensive review on models and standards. Urban Clim. 18, 33–57. https://doi.org/10.1016/j.uclim.2016.08.004.

Coffel, E.D., Horton, R.M., Sherbinin, A., 2018. Temperature and humidity based projections of a rapid rise in global heat stress exposure during the 21st century. Environ. Res. Lett. 13, 014001 https://doi.org/10.1088/1748-9326/aaa00e.

Dahinden, F., Fischer, E.M., Knutti, R., 2017. Future local climate unlike currently observed anywhere. Environ. Res. Lett. 12, 084004 https://doi.org/10.1088/1748-9326/aa75d7.

Davies-Jones, R., 2008. An efficient and accurate method for computing the wet-bulb temperature along pseudoadiabats. Mon. Weather Rev. 136, 2764–2785. https://doi.org/10.1175/2007MWR2224.1.

Déqué, M., 2007. Frequency of precipitation and temperature extremes over France in an anthropogenic scenario: Model results and statistical correction according to observed values. Global Planet. Change 57, 16–26. https://doi.org/10.1016/j.gloplacha.2006.11.030.

Ehret, U., et al., 2012. HESS Opinions "Should we apply bias correction to global and regional climate model data?". Hydrol. Earth Syst. Sci. 16, 3391–3404. https://doi.org/10.5194/hess-16-3391-2012.

Feigenwinter, I. et al., 2018. Exploring quantile mapping as a tool to produce user-tailored climate scenarios for Switzerland, Technical Report 270: MeteoSwiss.

Fischer, et al., 2022. Climate Scenarios for Switzerland CH2018 – approach and implications. Clim. Serv. 26, 100288 https://doi.org/10.1016/j.cliser.2022.100288.

Fischer, E.M., Oleson, K.W., Lawrence, D.M., 2012. Contrasting urban and rural heat stress responses to climate change. Geophys. Res. Lett. 39.

Fischer, E.M., Schär, C., 2010. Consistent geographical patterns of changes in high-impact European heatwaves. Nat. Geosci. 3, 398–403. https://doi.org/10.1038/ngeo866.

Fitzpatrick, M.C., Dunn, R.R., 2019. Contemporary climatic analogs for 540 North American urban areas in the late 21st century. Nat. Commun. 10, 614. https://doi.org/10.1038/s41467-019-08540-3.

Ford, J.D., et al., 2010. Case study and analogue methodologies in climate change vulnerability research. WIREs Clim. Change 1, 374–392. https://doi.org/10.1002/wcc.48.

García-León, D., Casanueva, A., Standardi, G., et al., 2021. Current and projected regional economic impacts of heatwaves in Europe. Nat Commun 12, 5807. https://doi.org/10.1038/s41467-021-26050-z.

Giorgi, F., Jones, C., Asrar, G., 2008. Addressing climate information needs at the regional level: The CORDEX framework. WMO Bull 53.

Glantz, M. H., 1991. The use of Analogies: In Forecasting Ecological and Societal Responses to Global Warming. Environment: Science and Policy for Sustainable Development, Volume 33, pp. 10-33. doi: 10.1080/00139157.1991.9931393.

Herger, N., Sanderson, B.M., Knutti, R., 2015. Improved pattern scaling approaches for the use in climate impact studies. Geophys. Res. Lett. 42, 3486–3494. https://doi.org/10.1002/2015GL063569.

Horton, R.M., et al., 2016. A review of recent advances in research on extreme heat events. Current Climate Change Reports 2, 242–259. https://doi.org/10.1007/s40641-016-0042-x.

Jacob, D., et al., 2014. EURO-CORDEX: new high-resolution climate change projections for European impact research. Reg. Environ. Change 14, 563–578. https://doi.org/10.1007/s10113-013-0499-2.

Jones, C., 2010. CORDEX: A coordinated regional downscaling experiment (Invited). AGU Fall Meeting Abstracts 12.

King, A.D., Karoly, D.J., 2017. Climate extremes in Europe at 1.5 and 2 degrees of global warming. Environ. Res. Lett. 12, 114031 https://doi.org/10.1088/1748-9326/aa8e2c.

Kjellstrom, T., et al., 2018. Estimating population heat exposure and impacts on working people in conjunction with climate change. Int. J. Biometeorol. 62, 291–306. https://doi.org/10.1007/s00484-017-1407-0.

Kjellstrom, Holmer, I., Lemke, B., 2009. Workplace heat stress, health and productivity –an increasing challenge for low and middle-income countries during climate change. Glob. Health Action 2. https://doi.org/10.3402/gha.v2i0.2047.

Klein Tank, A.M.G., et al., 2002. Daily dataset of 20th-century surface air temperature and precipitation series for the European Climate Assessment. Int. J. Climatol. 22, 1441–1453. https://doi.org/10.1002/joc.773.

Knutson, T.R., Ploshay, J.J., 2016. Detection of anthropogenic influence on a summertime heat stress index. Clim. Change 138, 25–39. https://doi.org/10.1007/s10584-016-1708-z.

Kotlarski, S., et al., 2014. Regional climate modeling on European scales: a joint standard evaluation of the EURO-CORDEX RCM ensemble. Geosci. Model Dev. 7, 1297–1333. https://doi.org/10.5194/gmd-7-1297-2014.

Kotlarski, S., 2019. SvenKotlarski/qmCH2018: qmCH2018 v1.0.1 (Version v1.0.1). Zenodo. http://doi.org/10.5281/zenodo.3275571.

Langner, M., Scherber, K. and Endlicher, W. R., 2014. Indoor heat stress: An assessment of human bioclimate using the UTCI in different buildings in Berlin. DIE ERDE – Journal of the Geographical Society of Berlin, 4, Volume 144, pp. 260-273. doi: 10.12854/erde-144-18.

Lemke, B., Kjellstrom, T., 2012. Calculating workplace WBGT from meteorological data. Ind. Health 50, 264–278. https://doi.org/10.2486/indhealth.ms1352.

Li, J., Chen, Y.D., Gan, T.Y., Lau, N., 2018. Elevated increases in human-perceived temperature under climate warming. Nat. Clim. Chang. 8, 43–47. https://doi.org/10.1038/s41558-017-0036-2.

Liang, C., et al., 2011. A new environmental heat stress index for indoor hot and humid environments based on Cox regression. Build. Environ. 46, 2472–2479. https://doi.org/10.1016/j.buildenv.2011.06.013.

Lin, W., Wang, C. Longer summers in the Northern Hemisphere under global warming. Clim Dyn 58, 2293–2307 (2022). https://doi.org/10.1007/s00382-021-06009-yMaraun, D. et al., 2017. Towards process-informed bias correction of climate change simulations. Nature Climate Change, 01 11, Volume 7, pp. 764-773. doi: 10.1038/nclimate3418.

Matthews, T., 2018. Humid heat and climate change. Prog. Phys. Geogr.: Earth Environ. 42, 391–405. https://doi.org/10.1177/0309133318776490.

Matthews, T. K. R., Wilby, R. L. and Murphy, C., 2017. Communicating the deadly consequences of global warming for human heat stress. Proc. Natl. Acad. Sci., doi: 10.1073/pnas.1617526114.

MeteoSwiss, 2021. Von den Warnungen bis zur Klimatologie – das Thema Hitze an der MeteoSchweiz. Zurich: Fachbericht MeteoSchweiz 276.

Moda, H.M., Filho, W.L., Minhas, A., 2019. Impacts of climate change on outdoor workers and their safety: some research priorities. Int. J. Environ. Res. Public Health 109, 163–179. https://doi.org/10.23749/mdl.v109i3.6851.

Mora, C., et al., 2017. Global risk of deadly heat. Nature Clim. Change 7, 501–506. https://doi.org/10.1038/nclimate3322.

Pal, J.S., Eltahir, E.A.B., 2016. Future temperature in southwest Asia projected to exceed a threshold for human adaptability. Nature Clim. Change 6, 197–200. https://doi.org/10.1038/nclimate2833.

Perkins, S.E., 2015. A review on the scientific understanding of heatwaves—Their measurement, driving mechanisms, and changes at the global scale. Atmos. Res. 164–165, 242–267. https://doi.org/10.1016/j.atmosres.2015.05.014.

Petitti, D.B., et al., 2016. Multiple trigger points for quantifying heat-health impacts: new evidence from a hot climate. Environ. Health Perspect. 124, 176–183. https://doi.org/10.1289/ehp.1409119.

Rohini, P., Rajeevan, M., Srivastava, A.K., 2016. On the variability and increasing trends of heat waves over India. Sci. Rep. 6, 26153. https://doi.org/10.1038/srep26153.

Seneviratne, S. I. et al., 2021. Weather and Climate Extreme. En: V. Masson-Delmotte, et al. edits. Climate Change 2021: The Physical Science Basis. Contribution of Working Group I to the Sixth Assessment Report of the Intergovernmental Panel on Climate Change. Cambridge University Press.

Sherwood, S.C., Huber, M., 2010. An adaptability limit to climate change due to heat stress. Proc. Natl. Acad. Sci. 107, 9552–9555. https://doi.org/10.1073/pnas.0913352107.

Skelton, M., Fischer, A.M., Liniger, M.A., Bresch, D.N., 2019. Who is 'the user' of climate services? Unpacking the use of national climate scenarios in Switzerland beyond sectors, numeracy and the research–practice binary. Clim. Serv. 15, 100113 https://doi.org/10.1016/j.cliser.2019.100113.

Smith, A., Lott, N., Vose, R., 2011. The integrated surface database: recent developments and partnerships. Bull. Am. Meteorol. Soc. 92, 704–708. https://doi.org/10.1175/2011BAMS3015.1.

Sørland, S., et al., 2020. CH2018 – National climate scenarios for Switzerland: How to construct consistent multi-model projections from ensembles of opportunity. Clim. Serv. 20, 100196.

Stull, R., 2011. Wet-bulb temperature from relative humidity and air temperature. J. Appl. Meteorol. Climatol. 50, 2267–2269. https://doi.org/10.1175/JAMC-D-11-0143.1.

Suarez-Gutierrez, L., Müller, W.A., Li, C., Marotzke, J., 2020. Hotspots of extreme heat under global warming. Clim. Dyn. 55, 429–447. https://doi.org/10.1007/s00382-020-05263-w.

UNDP, 2016. *Climate change and labour: impacts of heat in the workplace.* Issue paper. Geneva, CVF Secretariat, United Nations Development Program. http://www.undp.org/content/undp/en/ home/librarypage/climate-and-disaster-resilience-/tacklingchallenges- of-climate-change-and-workplace-heat-for-dev.html.

Vecellio, D.J., Wolf, S.T., Cottle, R.M., Larry Kenney, W., 2022. Evaluating the 35°C wet-bulb temperature adaptability threshold for young, healthy subjects (PSU HEAT Project). J. Appl. Physiol. 132 (2), 340–345. https://doi.org/10.1152/japplphysiol.00738.2021.

Vrac, M., Friederichs, P., 2015. Multivariate—intervariable, spatial, and temporal—bias correction. J. Climate 28, 218–237. https://doi.org/10.1175/JCLI-D-14-00059.1.

Wang J, Guan Y, Wu L et al (2021) Changing lengths of the four seasons by global warming. Geophys Res Lett 48:e2020GL091753. https://doi.org/10.1029/2020GL0917 53.

Wilcke, R.A.I., Mendlik, T., Gobiet, A., 2013. Multi-variable error correction of regional climate models. Clim. Change 120, 871–887. https://doi.org/10.1007/s10584-013-0845-x.

Willett, K.M., Sherwood, S., 2010. Exceedance of heat index thresholds for 15 regions under a warming climate using the wet-bulb globe temperature. Int. J. Climatol. 32, 161–177. https://doi.org/10.1002/joc.2257.

Xiang, J., Bi, P., Pisaniello, D., Hansen, A., 2014. Health impacts of workplace heat exposure: An epidemiological review. Ind. Health 52, 91–101. https://doi.org/10.2486/indhealth.2012-0145.

Yang, W., Gardelin, M., Olsson, J., Bosshard, T., 2015. Multi-variable bias correction: Application of forest fire risk in present and future climate in Sweden. *Nat. Harzards Earth System Sci.,* 9 15. https://doi.org/10.5194/nhess-15-2037-2015.

Zhao, Y., et al., 2015. Estimating heat stress from climate-based indicators: present-day biases and future spreads in the CMIP5 global climate model ensemble. Environ. Res. Lett. 10, 084013 https://doi.org/10.1088/1748-9326/10/8/084013.